Static Disorder Depth Profile in Ion Implanted Materials by Means of Large Angle Convergent Beam Electron Diffraction

Stefano Frabboni* and Francesca Gambetta

Istituto Nazionale Fisica della Materia (INFM) and Dipartimento di Fisica, Universita' di Modena, Via G. Campi 213/A, 41100 Modena, Italy

(Received 1 April 1998)

A new experimental method for static disorder depth profile in ion implanted crystalline materials is presented. Large angle convergent beam electron diffraction patterns of high angle reflections are used to directly compare, on a depth scale of the order of 10 nm, the integrated intensity coming from the undamaged crystal and from different slabs of the damaged layer. The case of high dose hydrogen implanted single crystal silicon wafers is studied. The results agree with the static disorder depth profile expected in both the as-implanted and the low temperature annealed samples. [S0031-9007(98)07270-6]

PACS numbers: 61.14.Lj, 61.43.–j, 61.72.Tt, 61.80.Jh

Static disorder in crystal structures arises from an irregular arrangement of atoms on the lattice sites or from the presence of vacancies and interstitial or impurity atoms; the determination of static disorder is therefore of great importance in the study of the physical properties of materials.

In the case of ion implanted materials static disorder is the structural parameter that describes the increase of radiation damage with the dose of impinging ions and the recovery of the crystalline structure after thermal treatments. The most widely used techniques for detecting static disorder are Rutherford backscattering channeling and double-crystal x-ray diffraction. Both techniques suffer a limited lateral spatial resolution and need accurate simulations in order to describe the static disorder depth profile in terms of the number of displaced atoms [1] or in terms of the atomic mean square displacement [2], respectively.

Despite the need of specimen thinning, the study of static disorder by convergent beam electron diffraction (CBED) seems promising. In fact, because of both the flatness of the Ewald sphere of 100 keV electrons and the angular convergence of the incident electron probe, high order reflections, characterized by a high sensitivity to the atomic displacements, can be excited from a very small volume of material [3].

In this Letter we present a new experimental method for the analysis of the static disorder based on the large angle convergent beam electron diffraction (LACBED) technique [4] available in a transmission electron microscope (TEM). In this technique a probe with a large convergence angle is focused in a plane slightly below the sample, thus forming a diffraction pattern (instead of an intermediate image) in the plane of the selected area aperture. This aperture can then be used to isolate one reflection and so prevent overlapping of the diffracted beams in the final detection plane. In these patterns different regions of the sample, with lateral dimensions of the order of the defocused probe diameter, contribute to different parts of the *same* diffraction pattern, thus allowing an accurate comparison between the diffracted intensity coming from different areas of the sample. In this way a *direct* measure of the static disorder versus depth with a spatial resolution of the order of 10 nm could be performed on cross sectioned samples by comparing the intensity diffracted by the perfect crystal with the one relative to different slices of the sample containing defects. The method we propose for intensity evaluation consists in estimating the ratio (*R ratio*) between *integrated intensity* in perfect crystal and in different slabs of implanted layer from dark field LACBED (DFLACBED) patterns.

Analyses have been carried out on TEM cross sections of ⟨100⟩ Si wafers implanted with H^+ ions of 15.5 keV at a dose of 1.6×10^{16} cm^{-2} keeping the sample at the liquid nitrogen temperature during the implantation. As it is known, this implantation produces small clusters of point defects characterized by a bell-shaped profile of Si displaced atoms centered at the H projected range [5]. In addition to the as-implanted sample some specimens annealed at 300 and 500 °C for 2 hours have been analyzed in order to observe the "reverse annealing" phenomena ascribed to the formation of small H_2 clusters dissolving at higher temperatures to form cavities [5]. The [1 −1 0] TEM cross sections have been prepared by dimpling and low angle ion milling with Ar^+ ions of 4 keV. A Philips EM400 (100 kV) have been used for TEM analyses; LACBED patterns have been digitally recorded by means of a 694 Gatan CCD slow scan camera with the microscope operating in nanoprobe mode (nominal spot size 10 nm), using a selected area aperture of 5 μm.

A study of crystal structures with defects based on the measurements of diffracted intensities needs the statement of a model for the calculation of the structure factors as crystallographic defects destroy the spatial periodicity of the crystal structure. When an average periodic lattice can be defined, the total scattered intensity distribution can be written as [6] $J^{tot}(s) = |\langle F(s)\rangle|^2 + |\langle \Delta F(s)\rangle|^2$. Here

s is the reciprocal lattice scattering vector, and $|\langle F(s)\rangle|^2$ is the square of the Fourier transform of the electrostatic potential $\langle V(r)\rangle$ of the average lattice which gives rise to the coherent intensity at the Bragg positions. The term $|\langle \Delta F(s)\rangle|^2$ represents the square of the Fourier transform of the deviation from the average lattice, $\langle \Delta V(r)\rangle$, which is, in general, a nonperiodic intensity (diffuse scattering). In the case of point defects or small aggregates of point defects each Fourier component of $\langle F(s)\rangle$, $\langle F_g\rangle$, can be expressed as $\langle F_g\rangle = F_g \exp[-L_H]$, where F_g is the structure factor of the crystal without defects corrected for the *thermal* Debye-Waller. The exponential factor is the so-called *static* Debye-Waller factor and is given by

$$L_H = 2\pi^2 g^2 \langle u^2\rangle_s , \qquad (1)$$

where $\langle u^2\rangle_s$ is the atomic mean square *static* displacement along the direction parallel to the reciprocal lattice vector $\mathbf{g}$. The correspondent reduction of the intensity in each diffracted beam increases the diffuse scattering with no broadening of the Bragg peak, thus determining a conservation of the total scattered intensity along each diffracted beam [6].

The experimental setup for the measurement of L_H in a (1 −1 0) TEM cross section is reported in Fig. 1. The sample is tilted toward the [4 −4 1] zone axis where the high angle reflection $\mathbf{g} = 880$ can be brought into the Bragg position and the Bragg contour (defined as the loci of the Bragg peak in the DFLACBED pattern) quantitatively analyzed. This reflection is not sensitive to atomic displacements, $\mathbf{r}$, along both the [001] and [1 −1 0] directions normal to the free surfaces of the bulk sample and of the TEM cross section because the $\mathbf{g}\cdot\mathbf{r} = 0$ rule holds in the selected geometry. Unwanted effects on the diffracted intensity due to the stress relaxation and to the specimen preparation can then be reasonably minimized.

Even if the sample is oriented along the quite "sparse" [4 −4 1] zone axis, the reduction of the diffracted intensity due to L_H is not *a priori* predictable on the basis of a simple kinematical theory because of the well-known

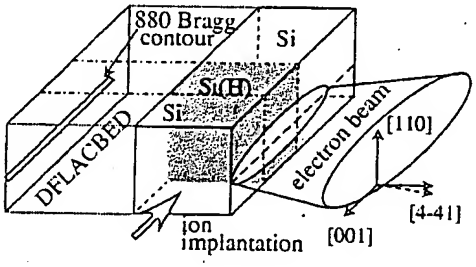

FIG. 1. Experimental setup for the measurement of static disorder in (1 −1 0) TEM cross sections. The [4 −4 1] zone axis is reached after a tilt of about 10° around the [110] direction. The dashed line is evidence of the trace of the (880) crystal planes crossing the interface between the defective layer and the undamaged crystal at right angle. The Bragg contour of this reflection ($g = 20.8$ nm^{-1}, two beam extinction distance 929 nm) has been used for the DFLACBED analysis.

many-beams character of the electron diffraction process. Therefore we have simulated the DFLACBED pattern solving the time-independent Schrödinger equation in the Bloch-wave formalism [7] for an electron probe of 100 keV with a half-convergence angle of 10 nm^{-1} impinging onto the specimen along the [4 −4 1] zone axis with the center of the Laue circle at $\mathbf{g} = 440$ ($\mathbf{g} = 880$ in Bragg position). Five silicon crystal structures with different levels of static disorder ($L_H^{(1)} = 0$, $L_H^{(2)} = 0.05$, $L_H^{(3)} = 0.15$, $L_H^{(4)} = 0.35$, $L_H^{(5)} = 0.85$, for $\mathbf{g} = 880$) have been considered. The calculations have been performed using the EMS software [8], including 15 zero-order Laue zone beams and 20 first-order Laue zone beams with maximum deviation parameter from the Bragg position $s_g^{\max} = 0.4$ nm^{-1}. Absorption has been taken into account using the Weikenmeier-Kohl scattering factor [9]. The integrated intensities have been calculated from line scans across the simulated Bragg contour. Convergence in the Bloch-wave calculations has been determined checking the invariance of the integrated intensities with respect to the increase of the number of the diffracted beams. In Fig. 2 are summarized the results of these calculations. It is shown [Fig. 2(a)] that the integrated intensity increases almost linearly with the thickness, t, of the sample for $t < 100$ nm as expected from the kinematical theory. For thicknesses greater than 225 nm the intensity reaches a plateau that increases in width as the static disorder increases. In Fig. 2(b) is reported the logarithm of integrated intensity versus the static disorder parameter L_H; it is shown that the integrated intensity, I_g, depends exponentially from $2L_H$, in the following way:

$$\frac{I_g(L_H, t)}{I_g^0(t)} = \exp[-2b(t)L_H], \qquad (2)$$

where $I_g^0(t)$ refers to the case of ordered structure, $L_H = 0$. The slope, $b(t)$, is equal to 1.14 and 1.2 for thicknesses of the sample equal to 25 and 100 nm, respectively. For thicknesses in the range 225–330 nm b is *nearly constant* and equal to 1.26. The values of $b(t)$, which are higher than the expected unitary value of the kinematical case, define the correction factor which must be applied to the logarithm of the intensity ratio reported in (2) in order to determine L_H in a "quasikinematical" approximation. It must be stressed here that the diffuse scattering intensity is not taken into account in the calculations. Nevertheless, according to Tsuda and Tanaka [10], we can suppose that for high angle reflections the contribution to the intensity of both the diffuse scattering and the inelastic scattering can be reasonably removed from the experimental patterns by linear background subtraction.

In Fig. 3(a) is reported a weak-beam TEM image of the as-implanted sample. The defects are located at a mean depth of about 210 nm (correspondent to the H-projected range) and form a band about 80 nm wide. The sample's local thickness has been determined from the analysis of

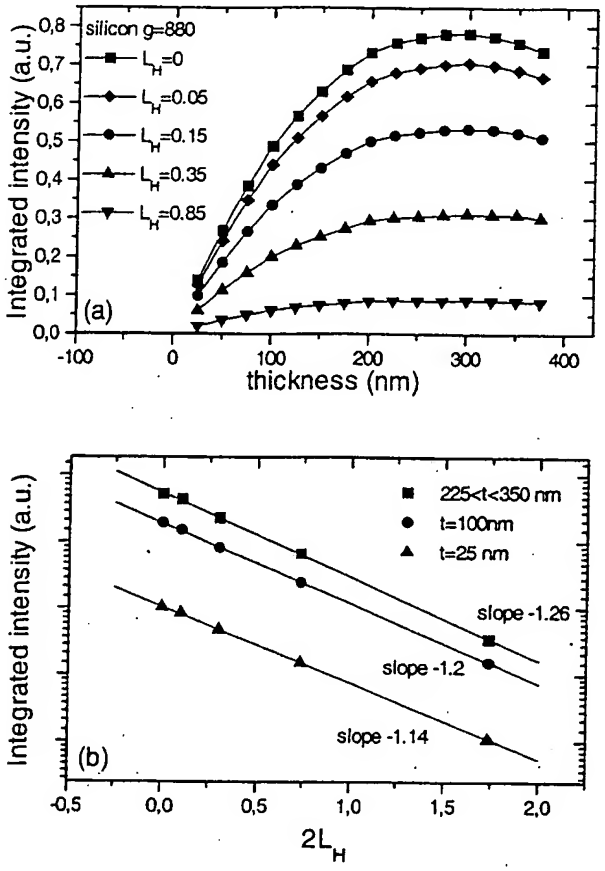

FIG. 2. (a) Integrated intensity vs thickness of the sample. Each point represents the integral under a line scan performed across a calculated 880 Bragg contour. (b) Logarithmic plot of the integrated intensity vs $2L_H$. Labels represent the slopes of the linear fit for different thicknesses of the sample.

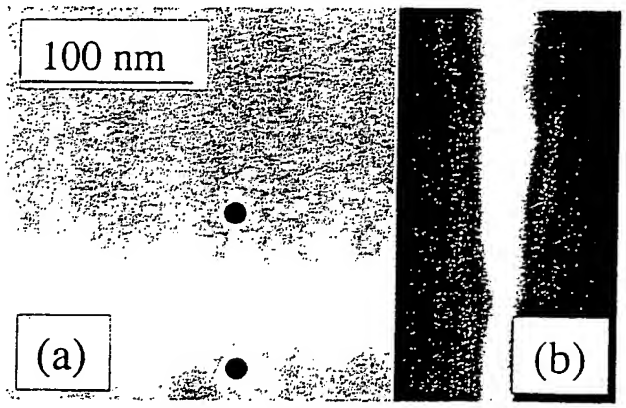

FIG. 3. (a) Weak-beam dark field TEM image [g = 220; (g, 2g)] of as-implanted specimen showing the defective layer due to H^+ implantation. Dots mark the areas where local thickness has been determined. (b) The 880 reflection DFLACBED. A loss of coherent diffracted intensity is evident in the defective region related to the crystallographic defects, hence to the static disorder. The upper edge of both figures corresponds to the surface of the specimen.

the CBED pattern of the **g** = 220 (not reported here) [7] obtained with the probe focused near the defective layer. A region with a local thickness between 250–300 nm ($b = 1.26$) has been selected to follow the proposed procedure for static disorder measurement. In Fig. 3(b) is reported the experimental DFLACBED pattern taken near the [4 −4 1] zone axis with the 880 Bragg contour. The depth scale can be calibrated by direct comparison with the diffraction contrast image of Fig. 3(a). As expected, the diffracted intensity increases with depth from the surface because of the wedge-shaped profile of the cross-section TEM sample, then decreases at the defects reaching a minimum at a depth of about 210 nm. In addition, the Bragg contour shows only a moderate shift at the Si/defective-layer interface; then a negligible stress relaxation along a direction parallel to **g** can be reasonably assumed. This fact induces us to mainly ascribe the loss of diffracted intensity to static disorder. Line scans taken across the Bragg contour in a region of the sample centered on the defective layer are reported in Fig. 4(a). It is evident that the intensity of the peak decreases monotonically reaching a minimum near the middle of the defective layer at a depth of 210 nm. On the contrary, at the deep side of the defective layer the intensity shows an increasing trend to the last sampled depth of 290 nm where the intensity reaches the local maximum. This is reasonable because at this depth the effect of the ion implantation on the crystal quality is negligible. In order to quantify the depth profile of the static disorder we have checked first the conservation of the total scattered intensity along the 880 reflection. We have evaluated the ratio $C(x) = J_{Si}/J(x)$, where x is the depth coordinate, J_{Si} and $J(x)$ are the integrated intensities measured under the line scan across the Bragg contour taken in the undamaged silicon (at a depth of about 290 nm) and in the defective layer (for x ranging between 150 and 280 nm), respectively. As shown in Fig. 4(b) (left scale, full circles) $C(x)$ is nearly constant and equal to one. This means that the selected area aperture used in the DFLACBED experiment to separate the diffracted beams does not produce an appreciable loss of the diffuse electron intensity caused by the mean absorption and/or by the diffuse scattering at the defective layer. Then after a linear background subtraction (the baseline of each intensity profile has been drawn connecting the intensity minima at both ends of each line scan), we have obtained the ratio $R(x) = I_{Si}/I(x)$ between the integrated intensity of the perfect silicon, I_{Si}, and of the different slabs in the defective layer, $I(x)$, respectively [Fig. 4(b), full square]. The evaluation of the $R(x)$ ratio allows us to determine the profile of L_H directly from (2) as the effect on the structure factor of strain (mainly uniaxial along the [001] and of the order of 5×10^{-3} [2]) and of the H concentration (lower than 3%) can be reasonably considered negligible with respect to the effect of L_H. The plot of L_H [Fig. 4(b), right scale] has the expected bell-shaped

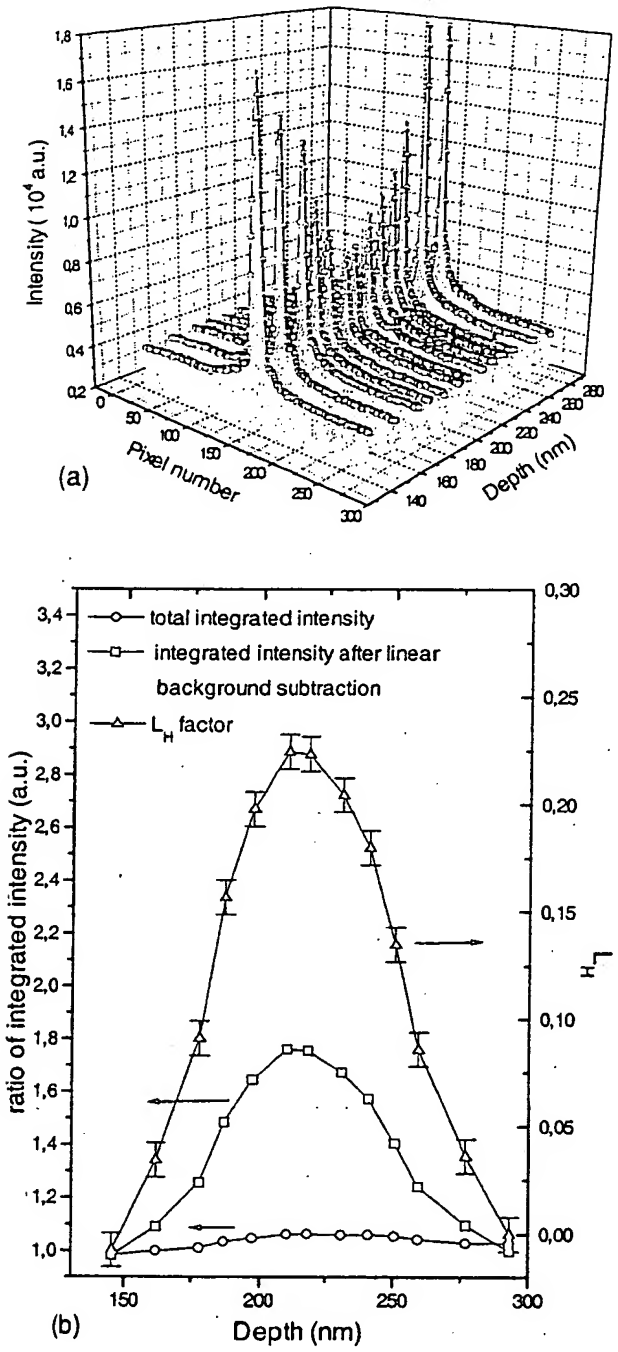

FIG. 4. (a) Experimental intensity profiles obtained from the line scans performed on the Bragg contour of Fig. 3(b). The gradual loss of coherent signal follows the damage implantation profile. (b) Left scale: Profiles of the ratio of total scattered intensity $C(x)$ (no background subtraction) and of the ratio $R(x)$ obtained after linear background subtraction. $C(x)$ ratio is almost constant over the range of depth analyzed; what changes is the $R(x)$ ratio because of the modified relationship between coherent and diffuse scattering at the defects. Right scale: Profile of L_H.

profile typical of the radiation damage induced by ion implantation. It is worth noting that the profile is drawn with a depth spatial resolution of 10–15 nm as suggested from the fact that the two points closest to the peak of L_H in Fig. 4(b) are almost indistinguishable, but certainly different, from their nearest neighbor.

The same procedure has been applied to the samples annealed at 300 and 500 °C for 2 hours. In these samples the values of $\langle u^2 \rangle_s$ measured at a depth of about 210 nm are equal to $(7.0 \pm 0.2) \times 10^{-5}$ nm^2 and $(3.3 \pm 0.1) \times 10^{-5}$ nm^2, respectively. These results, when compared with the as-implanted data ($\langle u^2 \rangle_s = (2.9 \pm 0.1) \times 10^{-5}$ nm^2), are consistent with the reverse annealing of radiation damage reported in the literature [2,5].

In conclusion, a new experimental method for evaluation of the depth profile of static disorder in ion implanted material with a 10 nm spatial resolution has been presented. In the working case of H implanted silicon the results, obtained using DFLACBED patterns of high angle diffracted beams, are in good agreement with literature data. The presented method could be extended to different types of samples, such as heterostructures and multilayers, and, in general, to thin films deposited on a substrate which can act as a reference for intensity measurement. The high spatial resolution attainable would open interesting perspectives in the field of semiconductor devices where the lateral dimensions of both the active and passive elements are continuously scaling down.

The authors are indebted to Dr. A. Armigliato and to Dr. R. Balboni, and to Professor G. Ottaviani, Dr. F. Corni, and Dr. R. Tonini for stimulating discussions.

*Author to whom correspondence should be addressed. Email address: frabboni@unimo.it

[1] J.F. Ziegler, J. Appl. Phys. **43**, 2973 (1972); G.F. Cerofolini *et al.*, Nuclear Instrum. Methods Phys. Res., Sect. B **71**, 441 (1992).
[2] R. Balboni, S. Milita, and M. Servidori, Phys. Status Solidi (a) **148**, 95 (1995).
[3] J. Taftø and T.H. Metzeger, J. Appl. Crystallogr. **18**, 110 (1985).
[4] M. Tanaka, J. Electron Microsc. **35**, 314 (1986).
[5] G.F. Cerofolini *et al.*, Phys. Rev. B **46**, 2061 (1992).
[6] J.M. Cowley, *Diffraction Physics* (North-Holland, Amsterdam, 1990).
[7] J.C.H. Spence and J.M. Zuo, *Electron Microdiffraction* (Plenum Press, New York and London, 1992).
[8] P.A. Stadelmann, Ultramicroscopy **21**, 131 (1987).
[9] A. Weikenmeyer and H. Khol, Acta Crystallogr. Sec. A **47**, 590 (1991).
[10] K. Tsuda and M. Tanaka, Acta Crystallogr. Sec. A **51**, 7 (1995).